Segment-specific targeting via RNA interference mediates down-regulation of OPN expression in hepatocellular carcinoma cells

F. Lin[1]*, C.M. Huang[2]*, J. Cao[1], Z.H. Pei[1], W.L. Gu[1], S.F. Fan[1], K.P. Li[1] and C.M. Lin[1]

[1]Department of General Surgery, Guangzhou First People's Hospital Affiliated to Guangzhou Medical University, Guangzhou, Guangdong, China
[2]Department of General Surgery, People's Hospital of Guangdong Province, Guangzhou, Guangdong, China

*These authors contributed equally to this study.
Corresponding author: J. Cao
E-mail: caojiecn@yeah.net

ABSTRACT. Osteopontin (OPN) plays an important role in the metastasis and recurrence of tumors after resection of hepatocellular carcinoma (HCC). In this study, the down-regulation effect on OPN expression in HCC cells of RNA interference (RNAi) molecules designed to target different segments of OPN was investigated to identify a more effective site for OPN knockdown. Specific small interfering RNAs (siRNAs A, B, and C) of *OPN* were synthesized and transfected into an HCC cell line (HEP-G2; representing the OPNi-A, OPNi-B, and OPNi-C groups). Fluorescent quantitative polymerase chain reaction and immunohistochemical methods were used to detect the mRNA and protein expression of OPN before and after RNAi. Results showed that after transfection, the fluorescence intensity of the OPNi-A group was greater than those of the OPNi-B and OPNi-C groups. After 48 h of transfection, the ΔCT values of *OPN* mRNA expression in the OPNi-

A-C groups increased from 8.31 ± 1.58, 8.78 ± 1.49, and 8.25 ± 1.51 to 12.14 ± 1.43, 10.22 ± 1.97, and 10.48 ± 1.88, respectively (P < 0.05), and the OPN protein levels (immunohistochemistry scores) decreased from 6.44 ± 1.67, 5.43 ± 2.05, and 5.45 ± 2.52 to 2.84 ± 1.52, 4.43 ± 1.65, and 3.95 ± 1.43 points, respectively. These results indicated that RNAi based on different segments of the *OPN* gene had different down-regulatory effects on OPN expression. Synthesis of targeted siRNA aimed at specific *OPN* segments might have important significance for dealing with the invasiveness and metastasis of HCC cells.

INTRODUCTION

Osteopontin (OPN) plays an important role in metastasis and recurrence of tumors after resection of hepatocellular carcinoma (HCC) (Qin and Tang, 2004; Tang et al., 2004; Bhattacharya et al., 2012). Most previous studies have examined the function of OPN (Chen et al., 2010; Lin et al., 2011; Liu et al., 2011). It has been found that OPN might be the molecular marker of hepatic metastasis as well as an important feedback factor of hepatic carcinoma. Angiogenesis is the foundation of malignant tumor invasion and metastasis. OPN exerts important functions in inducing angiogenesis in neurofibromatosis, multiple myeloma, and lung cancers during their invasion and metastasis processes. Although OPN promotion of tumor invasion and metastasis is not yet proven, the inter-reaction process between OPN and tumor metastasis-associated factors is still being researched and the status of OPN in the processes of malignant tumor formation, and especially of hepatic carcinoma invasion and metastasis, is as of yet undiscovered. OPN might take the role of ''molecular engine'' in these processes. Thus, the *OPN* gene sequence might be considered a key target for research, based upon its potential function in hepatic carcinoma invasion and metastasis. We think that, as there are protein domains of OPN, its segments might play key roles in its function. In this study, the effect of RNA interference on expressions of different OPN fragments in HCC was investigated. The objective of the study was to seek the most effective sequence for siRNA-mediated OPN knockdown, to provide a specific tool for use in the clinical therapy of HCC.

MATERIAL AND METHODS

Determination and synthesis of *OPN*-specific siRNA sequences

OPN was provided by Sigma Aldrich (St. Louis, MO, USA). With the assistance of PubMed (National Center for Biotechnology Information), the *OPN* mRNA sequence (NM 001040060.1) was retrieved, and three pairs of siRNA sequences were designed. The design principles were as follows: 1) the length of the siRNA was approximately 21-23 bp, with 2-3 nt at the 3'-end; 2) the target sequence was located at a site after 70-100 bp from the initiator ATG codon; 3) both initiator codons should be AA; 4) siRNAs were chosen with the lowest GC content (40-55%); 5) the primary structural region of the mRNA was avoided; 6) the uniqueness of the sequence was confirmed by BLAST homology comparison. The names and sequences of the *OPN* siRNAs are shown in Table 1.

Table 1. Names and sequences of *OPN*-specific siRNAs.

Name	siRNA base sequence	
	Sense (5'-3')	Antisense (5'-3')
siRNA A	CCU GUG CCA UAC CAG UUA AdTdT	UUA ACU GGU AUG GCA CAG GdTdT
siRNA B	GCU GUG UCC UCU GAA GAA AdTdT	UUU CUU CAG AGG ACA CAG CdTdT
siRNA C	GCA UCU UCU GAG GUC AAU UdTdT	AAU UGA CCU CAG AAG AUG CdTdT

Transfection of *OPN*-siRNA/Lipofectamine™ 2000 into cells

An aliquot consisting of 1.5 mL Opti-MEM® reduced-serum medium (Invitrogen Corp., CA, USA) was added to OPN-siRNA/Lipofectamine™ 2000 (Invitrogen Corp.), followed by transfection of siRNAs A-C into HEP-G2 cells (Liver Cancer Research Institute of Fudan University, Shanghai, China, according to manufacturer protocol), representing the OPNi-A, OPNi-B, and OPNi-C groups, respectively. Following transfection, cells were incubated with fresh serum-free medium (Fuzhou Maixin Biotechnology Development Co., Ltd., Fuzhou, China) (37°C, 5% CO_2) for 48 h. Finally, the cells were collected for identification and molecular biologic OPN detection assays. The experiments were conducted thrice.

Quantitative fluorescent polymerase chain reaction (PCR)

After 24, 36, and 48 h, total RNA was extracted from the cells, and quantitative fluorescent PCR was performed. The PCR amplification procedure was as follows: Stage 1 (predenaturation): 95°C for 30 s (1 cycle); Stage 2 (PCR): 95°C for 5 s, 60°C for 34 s (40 cycles); Stage 3 (dissociation): 95°C for 15 s, 60°C for 1 s, and 95°C for 15 s (1 cycle). The detection and analysis of RNA expression was as follows: 1.5 g agarose (Sigma-Aldrich Corp.) was added to 100 mL Tris-acetate-EDTA buffer (Nanjing MeiBo Biological Technology Co., Ltd., Nanjing, China) to prepare a 1.5% agarose gel. A 10-μL PCR product aliquot was added to 2 μL sample buffer, and the mixture was added to a well of the agarose gel. At the same time, the DNA marker (Shanghai Sangon Biological Engineering Technology & Services Co., Ltd., Shanghai, China) was added to a separate well on the agarose gel. Electrophoresis was performed at 80 V for 30-45 min. The agarose gel was placed in an ImageMaster VDS system (GE Healthcare Life Sciences, Piscataway, NJ, USA). The DNA bands were scanned and the integral optical density (IOD) value was analyzed. The IOD ratio of the target gene to the internal reference (*GAPDH*, Shanghai Sangon Biological Engineering Technology & Services Co., Ltd.,) reflected the relative expression amount of the target gene. The OPN mRNA expression was estimated using $2^{-\Delta\Delta Ct}$ method (Livak and Schmittgen, 2001).

Immunohistochemistry

Cells transfected with siRNA (OPNi-A, OPNi-B, and OPNi-C; 21, 21, and 16 samples in each group, respectively) were fixed with 4% polyformaldehyde for 40 min, and the sections were prepared. The sections were washed with phosphate-buffered saline (PBS), and then were treated with 0.3% Triton X-100/PBS. The specific mouse anti-human monoclonal OPN antibody (dilution 1:300; Santa Cruz Biotechnology Inc., Santa Cruz, CA, USA) was dropped on each section, followed by overnight incubation at 4°C. After three washes using

PBS of 3 min each, the secondary antibody Envision™ reagent (Envision Solar International Inc., San Diego, CA, USA) was dropped onto each section. The DAB staining was performed. The degree of coloring of each tissue section was observed under a microscope. The OPN antibody-positive paratonsillar cortex specimen was used as a positive control, and PBS instead of primary antibody was used as negative control.

Determination of results

Results were scored as 0-3 using a composite score method. The scoring according to coloring depth of the mucus in the cytoplasm or glandular cavity was as follows: light brown, 1; brown, 2; dark brown, 3; no coloration, 0. The scoring according to positive cell proportion was as follows: <30%, 1; 30-70%, 2; >70%, 3; no coloration, 0. The integration of above two scores was divided into 4 grades: score of 0, negative (-); 2-3, weak positive (+); 4, positive (++); 5-6, strong positive (+++). A score of over 4 represented over-expression.

Statistical analysis

Data are reported as means ± standard deviation. Statistical analysis was performed using the SPSS 13.0 statistical software (SPSS, Chicago, IL, USA). A *t*-test was used to analyze the differences among the three groups, and $P < 0.05$ was considered as statistically significant.

RESULTS

siRNA transfection efficiency

After 8 h from transfection of the siRNA A fragment into HEP-G2 cells, the green fluorescence of cells could be observed under an inverted microscope. The fluorescence intensity of the cells transfected with the A fragment was greater than those from the B and C fragments, respectively (Figures 1-3).
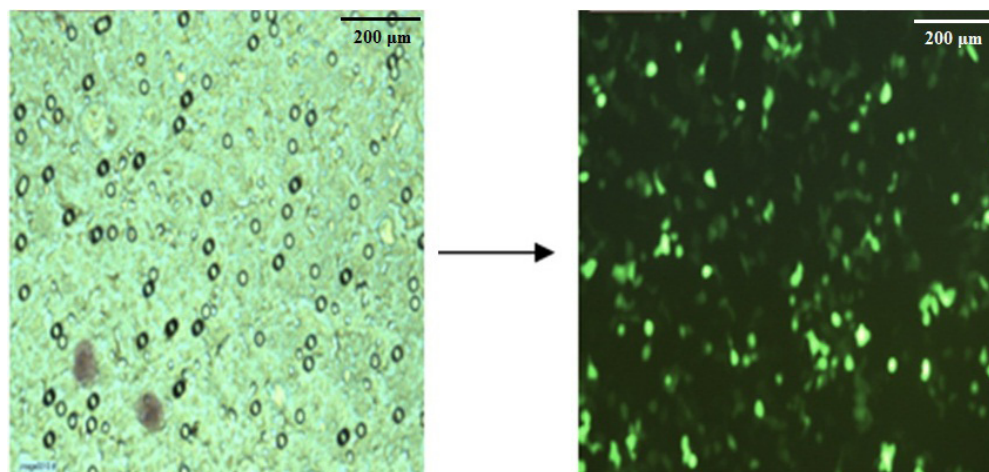

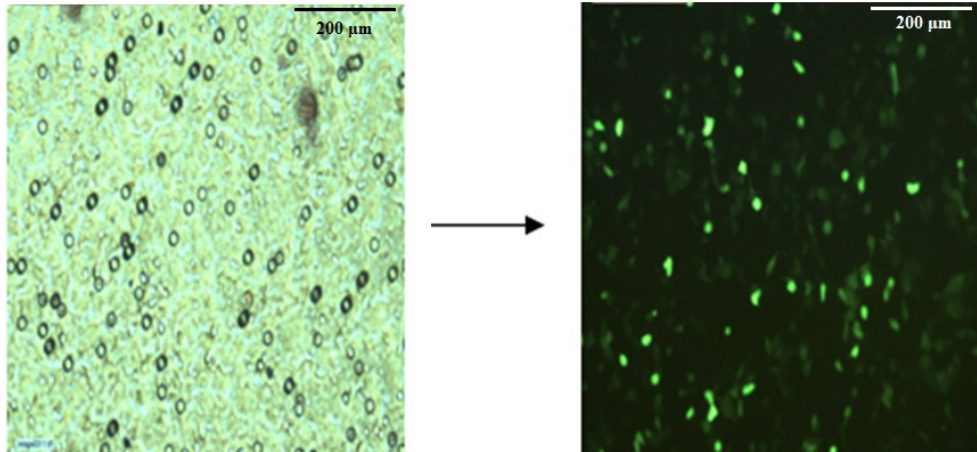**Figure 1.** A fragment transfected into HEP-G2 cells (200X).

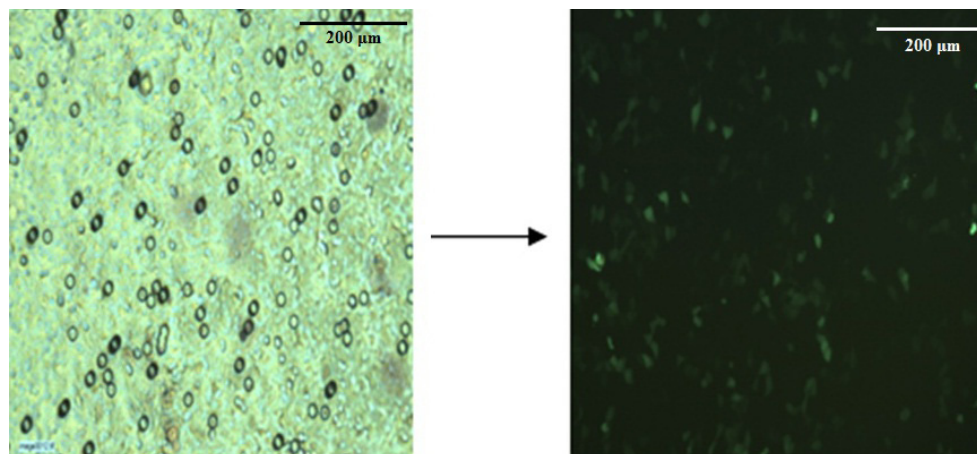**Figure 2.** B fragment transfected into HEP-G2 cells (200X).

Figure 3. C fragment transfected into HEP-G2 cells (200X).

Expression of *OPN* mRNA

Expression of *OPN* mRNA was represented by ΔCT (threshold cycle: the number of cycle of fluorescent signal reaching set threshold in each reaction tube). Results showed that there was a linear relationship between the initial copy number of each template and the template CT value. The larger the initial copy number, the smaller the CT value, and vice versa. Meanwhile, in order to observe the effect over time, the *OPN* RNA was collected at 24, 48, and 72 h after transfection, and the inhibition rate was detected. Results showed that 48 h after transfection, the ΔCT values of *OPN* mRNA expression in the OPNi-A, OPNi-B, and OPNi-C groups increased from 8.31 ± 1.58, 8.78 ± 1.49, and 8.25 ± 1.51 to 12.14 ± 1.43, 10.22 ± 1.97, and 10.48 ± 1.88, respectively ($P < 0.05$). These results suggested that the inhibitory rate of siRNA A on *OPN* mRNA expression was the strongest (Table 2).

Table 2. Expressions of OPN mRNA after interference (ΔCT) in the three groups.

Group	0 h	24 h	48 h	72 h	P
OPNi-A	1.01	10.68	12.14	9.84	
OPNi-B	1.04	9.82	10.22	9.13	<0.05*
OPNi-C	0.98	10.30	10.48	10.35	<0.05*

*OPNi-A group compared with OPNi-B and OPNi-C group.

Expression of the OPN protein

As shown in Table 3, the immunohistochemistry scores of OPN protein expression in OPNi-A, OPNi-B, and OPNi-C groups were 2.84 ± 1.52, 4.43 ± 1.65 and 3.95 ± 1.43 points, respectively. The protein expression level in the OPNi-A group was significantly lower than those in the OPNi-B and OPNi-C groups (P < 0.05).

Table 3. Expressions of OPN protein after interference in three groups.

Group	Number of sample	Immunohistochemistry score (IHS)	P
OPNi-A	21	2.84 ± 1.52	
OPNi-B	21	4.43 ± 1.65	<0.05*
OPNi-C	16	3.95 ± 1.43	<0.05*

*OPNi-A group compared with OPNi-B and OPNi-C group.

DISCUSSION

In this study, siRNAs against three segments of *OPN* were designed, and were transfected into HEP-G2 cells using Lipofectamine™ 2000. From the results, we found that the experimental data matched our expectations. The inhibitory rate of siRNA A on OPN expression was found to be stronger than siRNAs A and B. Segment A might represent a region of the mRNA more accessible to the siRNA; however, the exact mechanism of action still requires elucidation. If, through knockdown analysis, we can discover the nature of OPN function, which might be to serve as a trigger for metastasis and the recurrence of HCC (Wai and Kuo, 2008; Chen et al., 2011), this might contribute to better progress in the development of effective treatments for HCC.

Some researchers (Qin and Tang, 2004; Tang et al., 2004) have used genome and transcriptome technology to study the molecular genetic characteristics and gene expression profiles of surgical specimens from patients with HCC, metastatic human HCC xenografts in nude mice, and cell models and mechanisms of liver metastasis. After 10 years of concerted efforts, these studies have demonstrated that liver cancer metastasis-related gene changes already exist at the primary tumor stage. This has provided a new methodology for early diagnosis, treatment, and non-surgical intervention of HCC. It has also been confirmed that OPN is a key HCC metastasis-associated factor (Takafuji et al., 2007) and has a significant predictive value. This demonstration obtained the second prize in China's State Natural Science Award (the highest award in the medical field) in 2010, highlighting the importance of this finding.

siRNA molecules are short segments of double-stranded RNA (dsRNA) that can lock onto the complementary homologous mRNA sequences as their target goal and degrade them (Gotoh et al., 2002; Pan et al., 2007). The basic mechanism of RNAi is that dsRNA enters cells

and is sheared by intracellular dicer RNAse III and other dsRNA binding factors into 21-23 nt siRNAs. The siRNAs combine with certain proteins and enzymes (MUT-7, tRED-1, PAZ proteins, and DNA and RNA helicases) to form the RNA-induced silencing complex (RISC). Under the guidance of RNAi, RISC finds and identifies the complementary mRNA, and then the reverse strand of the siRNA combines with the helical structure of the RNA complex and the target mRNA, and shears the target mRNA. Thereby, the expression of the target gene is blocked, leading to gene silencing. RISC can also participate in another RNAi cycle (Tang et al., 2004). In this, RISC is positioned by base pairing to homologous mRNA transcripts, so that target gene transcription is blocked, generating the corresponding loss of functional phenotype. Therefore, this process has also been called posttranscriptional gene silencing (Qin and Tang, 2004; Celetti et al., 2005). RNAi technology has been widely applied to various fields in the life sciences, and is a revolutionary scientific development. In our previous studies (Seidman, 2002; de Silva Rudland et al., 2006), the structure and function of OPN have been studied in-depth. The results from those studies demonstrated that the molecular weight of OPN is small, but due to the complexity of the siRNA process, the synthesis of siRNA drugs for OPN has been very difficult with a high failure rate.

Therefore, we segmented the *OPN* nucleotide sequence and analyzed its more effective fragments, in order to synthesize more effective targeted siRNA molecules. The pre-examination of the RNA sequence can save more time and cost. In this paper, the siRNA molecules targeted to different *OPN* fragments were transfected into HEP-G2 cells, and the mRNA and protein levels of OPN were measured. These experiments demonstrated that all three fragments were able to down-regulate the expression of OPN, but fragment A led to the most obvious decreases. Therefore, siRNA A had the strongest effect, whereas siRNAs B and C were relatively weak. This might be related to specific sites in the sequence of siRNA A might have more sensitive reaction sites. In addition, the preferential effect might occur in conjunction with other factors involved in the modification process of *OPN* gene transcription and translation (Wai and Kuo, 2004; Robison and Lake, 2005; Teramoto et al., 2005). With a better understanding of the *OPN* molecular structure, the discovery of new tumor metastasis-associated factors related to OPN and of small molecule drugs for OPN might provide a turning point for the development of an effective gene therapy of HCC.

Conflicts of interest

The authors declare no conflict of interest.

ACKNOWLEDGMENTS

REFERENCES

Bhattacharya SD, Mi Z, Kim VM, Guo H, et al. (2012). Osteopontin regulates epithelial mesenchymal transition-associated growth of hepatocellular cancer in a mouse xenograft model. *Ann. Surg.* 255: 319-325.
Celetti A, Testa D, Staibano S, Merolla F, et al. (2005). Overexpression of the cytokine osteopontin identifies aggressive laryngeal squamous cell carcinomas and enhances carcinoma cell proliferation and invasiveness. *Clin. Cancer Res.* 11: 8019-8027.

Chen RX, Xia YH, Xue TC and Ye SL (2010). Transcription factor c-Myb promotes the invasion of hepatocellular carcinoma cells via increasing osteopontin expression. *J. Exp. Clin. Cancer Res.* 29: 172.

Chen RX, Xia YH, Xue TC and Ye SL (2011). Osteopontin promotes hepatocellular carcinoma invasion by up-regulating MMP-2 and uPA expression. *Mol. Biol. Rep.* 38: 3671-3677.

de Silva Rudland S, Martin L, Roshanlall C, Winstanley J, et al. (2006). Association of S100A4 and osteopontin with specific prognostic factors and survival of patients with minimally invasive breast cancer. *Clin. Cancer Res.* 12: 1192-1200.

Gotoh M, Sakamoto M, Kanetaka K, Chuuma M, et al. (2002). Overexpression of osteopontin in hepatocellular carcinoma. *Pathol. Int.* 52: 19-24.

Lin F, Li Y, Cao J, Fan S, et al. (2011). Overexpression of osteopontin in hepatocellular carcinoma and its relationships with metastasis, invasion of tumor cells. *Mol. Biol. Rep.* 38: 5205-5210.

Liu W, Xu G, Ma J, Jia W, et al. (2011). Osteopontin as a key mediator for vasculogenic mimicry in hepatocellular carcinoma. *Tohoku J. Exp. Med.* 224: 29-39.

Livak KJ and Schmittgen TD (2001). Analysis of relative gene expression data using real-time quantitative PCR and the $2^{-\Delta\Delta Ct}$ method. *Methods* 25: 402-408.

Pan HW, Ou YH, Peng SY, Liu SH, et al. (2007). Overexpression of osteopontin is associated with intrahepatic metastasis, early recurrence, and poorer prognosis of surgically resected hepatocellular carcinoma. *Cancer* 98: 119-127.

Qin LX and Tang ZY (2004). Recent progress in predictive biomarkers for metastatic recurrence of human hepatocellular carcinoma: a review of the literature. *J. Cancer Res. Clin. Oncol.* 130: 497-513.

Robison BW and Lake RA (2005). Advances in malignant mesothelioma. *N. Engl. J. Med.* 353: 1591-1603.

Seidman JD (2002). Osteopontin as a biomarker for ovarian cancer. *JAMA.* 287: 3209-3210.

Takafuji V, Forgues M, Unsworth E, Goldsmith P, et al. (2007). An osteopontin fragment is essential for tumor cell invasion in hepatocellular carcinoma. *Oncogene* 26: 6361-6371.

Tang ZY, Ye SL, Liu YK, Qin LX, et al. (2004). A decade's studies on metastasis of hepatocellular carcinoma. *J. Cancer Res. Clin. Oncol.* 130: 187-196.

Teramoto H, Castellone MD, Malek RL, Letwin N, et al. (2005). Autocrine activation of an osteopontin-CD44-Rac pathway enhances invasion and transformation by H-RasV12. *Oncogene* 24: 489-501.

Wai PY and Kuo PC (2004). The role of osteopontin in tumor metastasis. *J. Surg. Res.* 121: 228-241.

Wai PY and Kuo PC (2008). Osteopontin: regulation in tumor metastasis. *Cancer Metastasis Rev.* 27: 103-118.